Augmenting microgel flow *via* receptor-ligand binding in the constrained geometries of microchannels

Lindsey K. Fiddes,[a] Ho Ka Carol Chan,[a] Kristine Wyss,[bc] Craig A. Simmons,[bc] Eugenia Kumacheva*[a] and Aaron R. Wheeler*[ab]

Received 29th April 2008, Accepted 19th August 2008
First published as an Advance Article on the web 30th October 2008
DOI: 10.1039/b807106c

We investigated the flow dynamics of biotin-conjugated microgel capsules in avidin-conjugated microchannel constrictions. Microgels were prepared using a microfluidic assembly approach. Biotinylated microgels passing through avidin-modified constrictions slowed relative to several control systems. This effect was observed below a critical velocity of the microgels in the channel-at-large. The reduction in microgel velocity in the constriction occurred for several different sizes of microgels and orifices. Soft compliant microgels showed a lower velocity in the constriction relative to rigid microgels with the same concentration of biotin on the surface, due to the ability of the softer microgels to deform in the orifice and maximize their surface area when in contact with the orifice wall.

Introduction

Micrometre-size particles formed from polymer gels (microgels) possess a number of attractive features for applications in the pharmaceutical,[1–3] nutrition,[4–8] and cosmetic industries.[9–12] Microgel dimensions, structures, and chemical compositions can be readily controlled, making them highly versatile for a wide range of applications. In particular, microgels have been used as vehicles for drug delivery *via* the ocular, nasal, pulmonary, intratumoral, intramuscular, intravenous and transdermal pathways.[13–17] The effect of microgel size for each pathway has been well-studied; however, other factors such as the surface chemistry and mechanical properties are still being explored as means of increasing targeting of the microgel to the desired site.

Understanding the flow behavior of microgels in *in vivo*-like environments such as constrained geometries or in systems with strong particle-surface interactions is important for rationalizing and optimizing the efficiency of site-specific drug delivery. Furthermore, designing microgels with cell-like properties (*i.e.*, structure, size, compliance and surface chemistry) facilitates their use as a model system in studies of cells. Unlike cells, which are extremely heterogeneous, microgels can be precisely controlled, and their properties are constant within the timescale of experiments, so we can study their behavior in an appropriate and predictable way.

Microfluidics is a useful tool to study the relationship between the flow behaviors and adhesion properties of microscopic objects such as microgels or cells because an assortment of environments can be readily designed and constructed using a combination of microfabrication techniques and site-specific surface modification. Runyon *et al.*[18] studied the propagation of blood clotting in microchannels and found that using high shear rates lowered the concentration of molecular activators and prevented blood clotting. The authors examined cell confinement but did not extend their work to study cell-microchannel interactions.[18] Other research groups reported the use of microfluidics to study chemotaxis,[19,20] deformation,[21,22] sorting,[23,24] and infection[25] of cells. Theoretical work has shown that the effect of particle compliance, and mechanical and topographic patterns in channels, must be considered when developing new strategies for cell sorting.[26]

Recently, we reported the effect of electrostatic interactions on the flow of microgel capsules in constrained geometries.[27] We found that repulsion between the walls of microchannels and the capsules caused the microgels to move quickly through constrictions. In contrast, weak electrostatic attraction between the microgel capsules and the walls of microchannels had minimal effect on the velocity of microgels.

In the present paper, we describe the effect of receptor-ligand interactions on the flow of bioconjugated microgels in microchannels with dimensions comparable to the size of microgels, see Fig. 1(A). We used biotin-conjugated alginate microgels and avidin-conjugated microchannels as a model system. Increased concentration of biotin altered the velocities of the microgels as they passed through constrictions. The generality of these findings was confirmed by a series of control experiments. Furthermore, we explored the role of microgel compliance on flow behavior in topographically and chemically patterned microchannels.

Experimental

Fabrication of microfluidic devices

Microfluidic devices were fabricated in poly(dimethyl siloxane) (PDMS) by soft lithography[28] using a Sylgard 184 Silicone Elastomer Kit (Dow Corning Corp., Midland, MI). The microchannel was 150 μm deep and 1 mm wide, and contained a series

[a]*Department of Chemistry, University of Toronto, 80 St. George Street, Toronto, Ontario, Canada M5S 3H6. E-mail: ekumacheva@chem.utoronto.ca; awheeler@chem.utoronto.ca; Fax: (EK) +1 416 978 3576; (ARW) +1 416 946 3865; Tel: (EK) +1 416 978 3576; (ARW) +1 416 946 3864*
[b]*Institute of Biomaterials and Biomedical Engineering, University of Toronto, 164 College Street, Toronto, Ontario, Canada M5S 3G9*
[c]*Department of Mechanical and Industrial Engineering, University of Toronto, 5 King's College Road, Toronto, Ontario, Canada M5S 3G8*

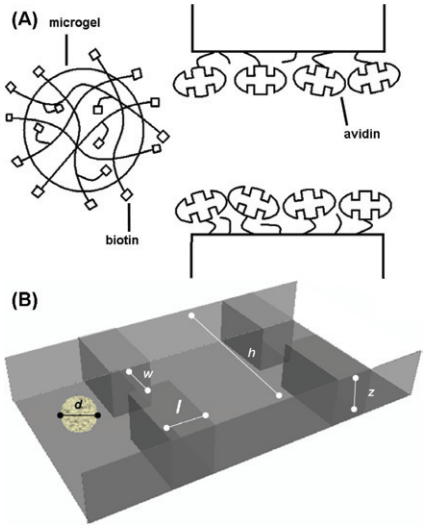

Fig. 1 Schematic of (A) a biotin-conjugated microgel entering an avidin-conjugated orifice, and (B) a multi-orifice channel. The diameter of microgel sizes, d, was 20, 30 and 40 μm in the experiments conducted in microfluidic devices with orifice widths, w, of 20, 30 and 40 μm, respectively. l = 75 μm, h = 1 mm.

of 30 equally spaced orifices with widths of 40, 30 and 20 μm (Fig. 1). The variation in orifice width was ± 5% RSD.

Site-specific patterning of microchannels

The surfaces of orifices in microchannels were modified *via* a two-step procedure. First, polyacrylamide (PAAm) was grafted to the surface of PDMS *via* site-specific photoinitiated graft-polymerization.[29] Second, the amide groups were functionalized with fluorescein isothiocyanate (FITC)-labeled avidin.[30–33]

All chemicals were purchased from Aldrich Canada and used as received. In the first step, a modification solution containing 17 wt% acrylamide, 9.7 wt% 2-butanol, 0.3 wt% benzophenone, 0.3 wt% Pluronic F-68, and 72.7 wt% deionized (DI) water was used. Prior to channel modification, the devices were incubated overnight in an oven at 75 °C. The microfluidic device was filled with the modification solution and the orifice regions were exposed to UV-radiation through a photomask (3 min, 200 mWatt/cm^2). Following UV-exposure, the microchannels were rinsed with deionized water and then filled and incubated (2 hr, RT) with a mixture of 1-ethyl-3-(3-dimethylaminopropyl)-carbodiimide (EDC) (5 mg/mL) and FITC-avidin (2.5 mg/mL) in 0.05 M phosphate buffer (pH = 7.0).[34] Following the incubation, the channels were rinsed again with DI water to remove excess FITC-avidin. The patterned microfluidic devices were stored in the dark at room temperature until use.

Fig. 2A–B shows representative bright-field and fluorescence microscopy images of a modified region in a microchannel. The fluorescence micrograph demonstrates good pattern fidelity. To confirm presence of the avidin on the surface, a planar PDMS substrate (with no topographical features) was modified in a separate experiment under identical conditions and characterized using FTIR spectroscopy (Bruker, Canada) using a Hyperion 15x reflection microscope with left exit detection. The signals from the background and sample were averaged over 32

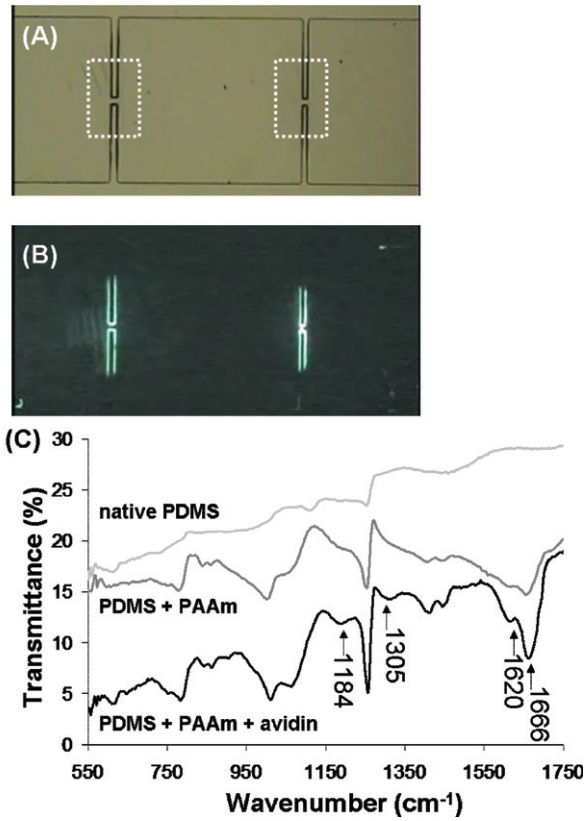

Fig. 2 Optical (A) and fluorescent (B) images of an orifice in a microchannel following attachment of FITC-avidin (top view). The dotted lines (A) indicate the area of PDMS exposed to UV radiation for graft-polymerization of PAAm. (C) FTIR spectra of non-modified PDMS, PDMS modified with PAAm, and PDMS modified with PAAm and conjugated with FITC-avidin.

scans in the range from 4000 to 400 cm^{-1} with a resolution of 4 cm^{-1}. Fig. 2C shows FTIR spectra of the bare PDMS, the PDMS modified with PAAm, and the PDMS modified with PAAm and functionalized with FITC-avidin. Peaks at 1666 and 1620 cm^{-1} are representative of the amide 1 and amide 2 stretches in PAAm.[35] The peaks at 1305 and 1184 cm^{-1} indicate the amide 3 and OH stretches in avidin.[36,37] The thickness of the dry PAAm layer was measured to be approximately 200 nm using a GETEST ellipsometer (Sopra, France).

Preparation of microgels

Prior to forming microgels, alginate was biotinylated using the method of Dhoot *et al.*[38] Briefly, sodium alginate powder was dissolved in 2-morpholino-ethane sulfonic acid (MES) buffer (0.1 M, pH 6.5) containing 0.3 M NaCl to a 2 wt% solution. Then, 0.05 g of EDC and 0.028 g of *N*-hydroxysuccinimide (NHS) were added and stirred for 15 min; 0.06 g of biotin was then added and stirred for 24 h. The solution was dialyzed for 4 days in 20 L of deionized water. After dialysis the solution was dilute, therefore the solution was evaporated to obtain a 2 wt% solution of alginate in the buffer. The weight ratio of biotin to alginate, α, was determined using an Optima 3000 inductively coupled plasma atomic emission spectrometer (ICP AES, Perkin

Elmer, UK). Solutions of 2 wt% alginate functionalized with 0 (non-modified alginate), 1.0, 3.0, 6.0, 7.3, and 17.0 wt% of biotin were prepared.

Biotinylated alginate was then used in the preparation of microgel capsules using the approach of Zhang *et al.*[39] Briefly, a 2 wt% aqueous solution of biotinylated alginate was emulsified in a microfluidic flow-focusing device and gelled *in situ* with Ca^{2+}-ions to produce microgel capsules.[40] Particles were transferred from the oil to a solution of 0.01 M phosphate buffer (pH 7.4) by centrifugation at 500 rpm for 10 min. Optical microscopy images were collected and analyzed using a light microscope (Olympus BX51) with a high-speed camera (Olympus U-CMAD3) and Image Pro Plus software (Media Cybernetics, Silver Springs, MD, USA). The polydispersity of the microgels (determined as coefficient of variation) was below 5%.

Mechanical properties of the microgel capsules were evaluated using the micropipette aspiration (MA) technique, as described by Hochmuth.[41] The instantaneous shear moduli of the microgel capsules were determined by fitting experimental force-deformation data to a numerically-derived model that accounts for large deformation and gel and pipette geometries.[42]

Experimental design

We examined the flow characteristics of non-modified alginate microgels and biotinylated alginate microgels. Dispersions of microgels (50 000 mL^{-1}) were introduced into the microchannel *via* polyethylene tubing connected to a reservoir. Fluid velocity was controlled by varying the height of the feeding reservoir (which was mounted on a vertical translation stage) with respect to the height of the microchannel. Unless specified, microgel velocities in the channels-at-large (outside the orifices) were kept at 125 $\pm$ 15 μm s^{-1}. The total residence time of the swollen microgel in the channel was 4 min, which is significantly shorter then the time it takes microgel particles to sediment.

The motion of the microgels through orifices was monitored under 200 $\times$ magnification. To determine linear velocities of microgels, the microchannel was divided into 13.4 μm-wide regions aligned perpendicular to the direction of fluid flow. The velocity of microgel particles was determined in each region and plotted as a function of the distance from the centre of the orifice (taken as the origin). For every experimental condition, the velocity profiles of the microgels were normalized with respect to their velocity in the channel-at-large (calculated as the average of the velocities measured in the region of 281 $\pm$ 27 μm from the center of the orifice). The normalized velocity profiles were averaged for at least 50 microgel particles.

Results and discussion

Flow characteristics of the microgels

In the present work, we studied the flow of biotinylated microgels with three diameters, 40, 30 and 20 μm, through avidin-modified orifices with matching widths (*i.e.*, 40, 30 and 20 μm). We also evaluated two control systems: non-modified alginate microgels with avidin-modified orifices, and biotinylated microgels with non-modified orifices. The microgels had a density similar to that of the phosphate buffer, and their diameters were significantly smaller than the height of the microchannels. Thus we assumed that the microgels flowed in the center of the channels without touching the top or bottom surfaces.

We first examined the flow of microgels in native PDMS channels. Fig. 3(A) shows the normalized velocity profiles of 40 μm-diameter microgels traveling through 40 μm-wide non-modified orifices. We denoted the average microgel velocity in the orifice region of the velocity profile, as the maximum normalized velocity, v_{max}. We found that the values of v_{max} of all microgels ranged from 9.6 $\pm$ 2.0 for $\alpha = 10$ wt% to 10.6 $\pm$ 1.7 for $\alpha = 17$ wt%. A paired t-test of these data indicated that there were no significant differences between the populations ($P = 0.31$). Thus, we conclude that no specific interactions between the microgels and orifice surface occurred in the control system.

Fig. 3(B) shows the normalized velocity profiles of 40 μm-diameter microgels traveling through 40 μm-wide avidin-modified orifices. The values of v_{max} of the microgels with $\alpha = 0$ and 1.0% were 12.2 $\pm$ 2.0 and 11.5 $\pm$ 1.8, respectively. The similarity of these data to each other and to those in Fig. 3(A) suggested that 1.0% biotinylation did not have a notable effect on the flow behavior. In contrast, the values of v_{max} of microgels with α of 3.0, 6.0, 7.3, and 17.0 wt% were 6.5 $\pm$ 0.9, 5.5 $\pm$ 1.2, 5.4 $\pm$ 1.1, and 5.0 $\pm$ 1.1, respectively. These data suggest that the addition of biotin to alginate in amounts equal to or exceeding 3% is sufficient to cause specific avidin-biotin interactions between the microgels and the surfaces, which slows them as they flow through the orifices. There is no significant difference between the flow of microgels with α of 3.0, 6.0, 7.3, and 17.0 wt%. This indicates that the available avidin binding sites on the orifice surface are used to their maximum capacity at α equal to

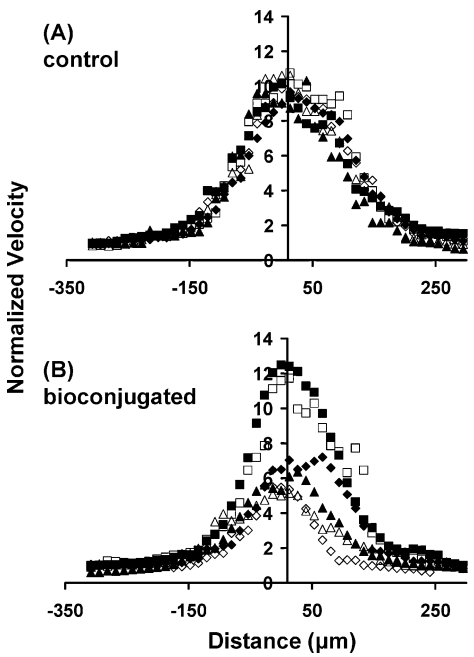

Fig. 3 Experimentally measured profiles of normalized velocity of 40 μm-diameter microgels at α, wt%: 0 (■), 1.0 (□), 3.0 (◆), 6.03 (◇), 7.3 (▲), and 17.0 (Δ) flowing through: (A) a 40 μm-wide orifice of non-modified PDMS; and (B) a 40 μm-wide orifice conjugated with FITC-avidin.

3.0 wt%, therefore when α is greater then 3% the additional biotin ligands cannot be used to slow the flow of the microgel.

A second notable difference between microgels formed with low (0–1 wt%) and high ($\geq$3 wt%) levels of biotin was the shape of the velocity profiles: the latter population had velocity profiles with flat maxima, while the former had sharper peak-shapes. The flat shape, indicating constant intra-orifice velocity, agrees with the computational model of the flow of a compliant capsular particle through an orifice of comparable dimensions.[43] This feature provided additional evidence of interactions between the orifice and the microgel surfaces.

Effect of initial velocity of the microgels on flow profile

We examined the effect of initial velocity on the flow characteristics of 40 μm-diameter microgels comprising 17.0 wt% of biotin in microchannels with 40 μm-wide avidin-modified orifices. To study this effect, we determined the normalized maximum velocities, ν_{max} (bio) and ν_{max} (non-bio), corresponding to the biotinylated and the non-modified alginate microgels, respectively. Fig. 4 shows the variation in $\Delta\nu_{max} = [\nu_{max}$ (non-bio) $- \nu_{max}$ (bio)]/ν_{max} (bio), plotted as a function of the initial velocity of microgels. Under forced flow, up to initial velocity of *ca.* 170 μm/s, biotin-avidin interactions were sufficiently strong to affect the motion of the microgels. As flow rates were increased, the effects of specific interactions on the velocities of the microgels (relative to the control system) decreased, and at a microgel initial velocity exceeding 200 μm s^{-1} negligible differences in microgel flow were observed.

Effect of size on microgel-orifice interactions

To demonstrate the generality of the observed trends, we evaluated two other systems in which the diameters of microgels were commensurate with the widths of the orifices. Fig. 5 shows the variation in ν_{max} for 20, 30, and 40 μm-diameter microgels plotted as a function of biotin concentration in the alginate polymer. For all microgel particles two flow regimes were observed: a fast flow regime, for microgels in which the biotinylation was less than 1 wt%, and a slow flow regime in which biotinylation of microgels was greater than 3 wt%. In the slow flow regime, the interactions between the microgels and the surface were presumably determined by the number of avidin functional groups on the surface of the orifice, so that they did not change at increasing degree of biotinylation.

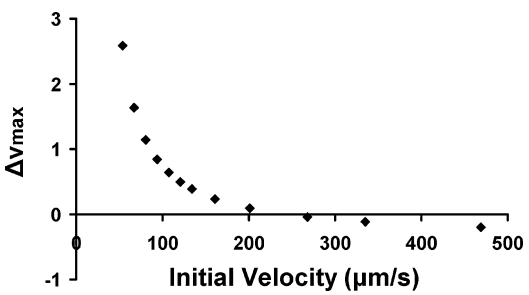

Fig. 4 The dependence of $\Delta\nu_{max}$ on the initial velocity of the microgel. $\Delta\nu_{max}$ was calculated as $[\nu_{max}$ (non-bio) $- \nu_{max}$ (bio)]/ν_{max} (bio). The diameter of microgels is 40 μm.

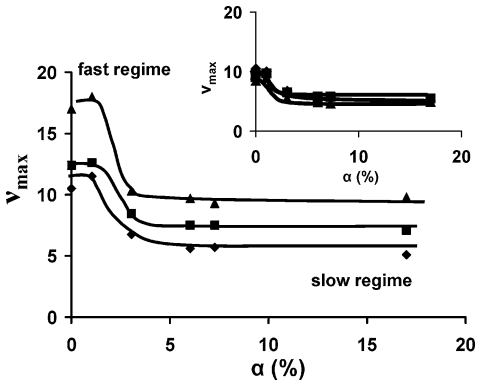

Fig. 5 The dependence of ν_{max} on the variation in α for 40 μm-wide (◆), 30 μm-wide (■), and 20 μm-wide (▲) orifices. Inset: variation in ν_{max} scaled to the change in fluid velocity in the orifice. Lines are added to guide the eye.

We note that a difference between the values of maximum normalized velocities of three types of microgels was observed, which was explained as follows. As fluid travels from the 1000 μm-wide upstream channel to an orifice with a width of 40, 30, or 20 μm, the velocity of the fluid is expected to undergo a 25, 33, and 50-fold increase, respectively (which is related as 1 : 4/3 : 2). Accordingly, the value of ν_{max} of microgels dispersed in the fluid should exhibit a similar trend. Fig. 5 (inset) shows ν_{max} for 40, 30, and 20 μm-sized microgels after normalization by 1 : 4/3 : 2, respectively. As shown, the difference between the flow of the microgels in the different size regimes was negligible. This result suggests that the biospecific interactions between the microgels and the walls of the channels scales with changes in velocity, and that the variation in the flow properties of microgels can be generalized for constrictions with dimensions commensurate with microgel size.

Effect of the mechanical properties of microgels

Soft objects such as microgels or cells do not follow streamlines when they pass through constrictions, as rigid particles do.[44] When soft particles pass through constrictions, the shear deforms these objects, which causes drift towards the center of the channel, a phenomenon termed as the Fahraeus effect.[45] To examine the effect of deformability of microgels, we tuned their compliance by varying the crosslinking density of alginate in the microgel particles. We prepared two types of 40 μm-diameter microgels which contained 1 and 4 wt% of biotinylated alginate to evaluate the effect of microgel compliance on the maximum normalized velocity in a 40 μm-wide orifice. The normalized velocity profiles of these microgels are shown in Fig. 6. The soft microgels (shear moduli of 1.63 kPa) had ν_{max} of 7.3 $\pm$ 1.4, while the rigid microgels (with shear moduli 2.99 kPa), had a ν_{max} of 14.4 $\pm$ 1.3. A paired t-test of these data indicated that there was a significant difference between the populations ($P = 0.00014$). We conclude from this data that increasing the rigidity of biotinylated microgels decreases the extent to which they deform in the orifice in the direction of flow and therefore decreases the area of contact of the microgels with the avidin-modified surface of the orifice.

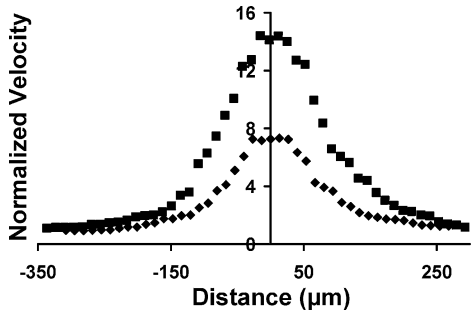

Fig. 6 Experimentally measured profiles of normalized velocity of 40 μm-diameter rigid (■) and soft (◆) biotinylated microgels passing through a 40 μm-wide orifice modified with avidin.

Conclusions

We report the results of experiments exploring the effect of receptor-ligand interactions in confined geometries under forced flow. The extent of these interactions was probed by measuring the velocity profile of the microgels in the microchannel orifices. Biotin/avidin interactions caused the microgels to move slowly, in comparison with control systems (lacking modification of the microgel or the surface of the orifice). In addition, the velocity profiles of the modified microgels flowing through functionalized orifices were flattened, indicating such that the microgels had constant velocities. The effect of the biotin-avidin interactions on the microgel flow depended on the initial velocities of the microgels in the microchannel-at-large: the interaction had the greatest effect when the initial velocity was slow. These results are an important first step in evaluating the manipulation of flow of soft particles experiencing receptor-ligand binding which we expect to be useful for a wide range of applications.

Acknowledgements

The authors are grateful to Prof. Anna Balazs for fruitful discussions. The authors thank Canada Research Chair fund for financial support.

References

1 S. V. Vinogradov, *Curr Pharm Des*, 2006, **12**, 4703–12.
2 H. Zhang, S. Mardyani, W. C. Chan and E. Kumacheva, *Biomacromolecules*, 2006, **7**, 1568–72.
3 M. Das, S. Mardyani, W. C. Chan and E. Kumacheva, *Adv Mater*, 2006, **18**, 80–3.
4 R. Czechowska-Biskup, P. Ulanski, A. K. Olejnik, G. Nowicka, B. Panczenko-Kresowska and J. M. Rosiak, *J Appl Polym Sci*, 2007, **105**, 169–176.
5 J. S. Mounsey, B. T. O'Kennedy, P. M. Kelly, L. Pesquera and J. C. Jacquier, *Special Publication - Royal Society of Chemistry*, 2006, **303**, 257–67.
6 J. de Vicente, J. R. Stokes and H. A. Spikes, *Food Hydrocolloids*, 2006, **20**, 483–91.
7 A. A. Khan, H. M. Khan and H. Delincee, *Food Control*, 2005, **16**, 141–6.
8 M. Villarini, G. Scassellati-Sforzolini, M. Moretti and R. Pasquini, *Cell Biol Toxicol*, 2000, **16**, 285–92.
9 V. C. Lopez, J. Hadgraft and M. J. Snowden, *Int J Pharm*, 2005, **292**, 137–47.
10 O. Popanda, R. Ebbeler, D. Twardella, I. Helmbold, F. Gotzes, P. Schmezer, H. W. Thielmann, D. von Fournier, W. Haase, M. L. Sautter-Bihl, F. Wenz, H. Bartsch and J. Chang-Claude, *Int J Radiat Oncol Biol Phys*, 2003, **55**, 1216–25.
11 R. Rigoletto, Y. Zhou and L. Foltis, *J Cosmet Sci*, 2007, **58**, 451–76.
12 S. Saxena, S. Nacht, *Delivery System Handbook for Personal Care and Cosmetic Products*, 2005, 333-351.
13 H. O. Alpar, S. Somavarapu, K. N. Atuah and V. W. Bramwell, *Adv Drug Del Rev*, 2005, **57**, 411–30.
14 B. Elmas, M. Tuncel, S. Senel, S. Patir and A. Tuncel, *J Colloid Interface Sci*, 2007, **313**, 174–83.
15 T. Hoare and R. Pelton, *Langmuir*, 2008, **24**, 1005–12.
16 A. Z. Pich and H.-J. P. Adler, *Polym Int*, 2007, **56**, 291–307.
17 Y. Tabata, Y. Murakami and Y. Ikada, *J Controlled Release*, 1997, **50**, 123–33.
18 M. K. Runyon, B. L. Johnson-Kerner, C. J. Kastrup, T. G. Van Ha and R. F. Ismagilov, *J Amer Chem Soc*, 2007, **129**, 7014–5.
19 S. Kanegasaki, Y. Nomura, N. Nitta, S. Akiyama, T. Tamatani, Y. Goshoh, T. Yoshida, T. Sato and Y. Kikuchi, *J Immunol Methods*, 2003, **282**, 1–11.
20 G. Walker, M. J. Sai, A. Richmond, M. Stremler, C. Y. Chung and J. P. Wikswo, *Lab Chip*, 2004, **5**, 611–8.
21 Y. Kikuchi, Q.-W. Da and T. Fujino, *Microvas Res*, 1994, **47**, 222–31.
22 J. P. Shelby, J. White, K. Ganesan, P. K. Rathod and D. T. Chiu, *Proc Natl Acad Sci*, 2003, **100**, 14618–22.
23 L. M. Barrett, A. J. Skulan, A. K. Singh, E. B. Cummings and G. J. Fiechtner, *Anal Chem*, 2005, **77**, 6798–804.
24 U. Kim, C.-W. Shu, K. Y. Dane, P. S. Daugherty, J. Y. Wang and H. T. Soh, *Proc Nal Acad Sci*, 2007, **104**, 20708–12.
25 G. M. Walker, M. S. Ozers and D. J. Beebe, *Sens Actuators B*, 2004, **98**, 347–55.
26 A. Alexeev, R. Verberg and A. C. Balazs, *Macromolecules*, 2005, **38**, 10244–60.
27 L. K. Fiddes, E. W. K. Young, E. Kumacheva and A. R. Wheeler, *Lab Chip*, 2007, **7**, 863–7.
28 Y. N. Xia and G. M. Whitesides, *Angew Chem Int Ed*, 1998, **37**, 551–75.
29 T. Rohr, D. F. Ogletree, F. Svec and J. M. J. Frechet, *Adv Funtc Mater*, 2003, **13**, 264–70.
30 H. Rinderknecht, *Nature*, 1962, **193**, 167–8.
31 S. Y. Yang, D. Lee, R. E. Cohen and M. F. Rubner, *Langmuir*, 2004, **20**, 5978–81.
32 Z. Li, D. Lee, M. F. Rubner and R. E. Cohen, *Macromolecules*, 2005, **38**, 7876–9.
33 D. Lee, M. F. Rubner and R. E. Cohen, *Chem Mater*, 2005, **17**, 1099–105.
34 C. Situma, A. J. Moehring, M. A. F. Noor and S. A. Soper, *Anal Biochem*, 2007, **363**, 35–45.
35 M. A. Moharram, S. M. RAbie and H. M. El-Gendy, *J Appl Polym Sci*, 2002, **85**, 1619–23.
36 R. Barbucci, A. Magnani, C. Roncolini and S. Silvestri, *Biopolymers*, 1991, **31**, 827–34.
37 Y.-S. Kim, J.-H. Cho, S. G. Ansari, H.-I. Kim, M. A. Dar, H.-K. Seo, G.-S. Kim, D.-S. Lee, G. Khang and H.-S. Shin, *Synth Met*, 2006, **156**, 938–43.
38 N. O. Dhoot, C. A. Tobias, I. Fischer and M. A. Wheatley, *Wiley InterScience*, 2004, 191–6.
39 H. Zhang, E. Tumarkin, R. Peerani, Z. Nie, R. M. A. Sullan, G. C. Walker and E. Kumacheva, *J Amer Chem Soc*, 2006, **128**, 12205–10.
40 S. L. Anna, N. Bontoux and H. A. Stone, *Appl Phys Lett*, 2003, **82**, 364–6.
41 R. M. Hochmuth, *J Biomech*, 2000, **33**, 15–22.
42 E. H. Zhou and C. T. Lim, *Mech Ad Mater Struct*, 2005, **12**, 501–12.
43 G. Zhu, A. Alexeev, E. Kumacheva and A. C. Balazs, *J Chem Phys*, 2007, **127**, 034701-034701-034710.
44 M. A. Faivre, K. Bickraj and H. A. Stone, *Biorheology*, 2006, **43**, 147159.
45 R. Fahraeus, *Physiol Rev*, 1929, **9**, 241–74.

